ELECTROWEAK STUDIES AND SEARCHES IN INCLUSIVE HIGH Q^2 ep COLLISIONS

Stefan Schmitt
DESY, Notkestraße 85, 22607 Hamburg, Germany

Recent results from the analysis of inclusive high Q^2 collisions of longitudinally polarised electrons or positrons and protons recorded at HERA are presented. The data are used to measure electroweak parameters and to search for new physics beyond the standard model.

1 Introduction

The HERA machine and the two collider experiments H1 [1] and ZEUS [2] have been taking data since 1992. Since 2003 both experiments have upgraded interaction regions including strong focusing magnets, and the instantaneous luminosity has increased by a factor 3. Furthermore, spin rotators have been added near H1 and ZEUS, leading to collisions of protons with longitudinally polarised electrons or positrons. The machine operates at a centre-of-mass energy $\sqrt{s} = 320\,\mathrm{GeV}$. The inclusive cross-sections presented here are measured in two reactions: neutral current (NC) and charged current (CC) interactions. For NC interactions, the scattered electron is detected in the tracking systems and the calorimeter. In contrast, CC interactions involve a scattered neutrino, which escapes detection. The kinematics of the scattering process is determined by the negative square of the momentum transfer, Q^2, the proton momentum fraction of the struck quark Bjorken, x, and the inelasticity, y. These observables are related by $Q^2 = sxy$, so only two of them are independent.

1.1 The Neutral Current Cross-Section

The NC inclusive cross-sections may be written in terms of the polarisation dependent generalised structure functions $\tilde{F}_2$, $x\tilde{F}_3$, $\tilde{F}_L$,

$$\frac{d^2\sigma^{NC}}{dx\,dQ^2} = \frac{2\pi\alpha^2}{xQ^4}\left[Y_+\tilde{F}_2(x,Q^2) \mp Y_- x\tilde{F}_3(x,Q^2) - y^2\tilde{F}_L(x,Q^2)\right].$$

The $\mp$ sign in front of the $x\tilde{F}_3$ term corresponds to the case of $e^{\pm}p$ scattering. The helicity functions are defined as $Y_\pm = 1 \pm (1-y)^2$. The contribution from $\tilde{F}_L$ is small and can be neglected at high Q^2. The generalised structure functions $\tilde{F}_2$ and $x\tilde{F}_3$ can be expressed as:

$$\tilde{F}_2 = F_2 - (v_e \pm P_e a_e)\kappa\frac{Q^2}{Q^2+M_Z^2}F_2^{\gamma Z} + (v_e^2 + a_e^2 \pm P_e 2v_e a_e)\kappa^2\left[\frac{Q^2}{Q^2+M_Z^2}\right]^2 F_2^Z,$$

$$x\tilde{F}_3 = -(a_e \pm P_e v_e)\kappa\frac{Q^2}{Q^2+M_Z^2}xF_3^{\gamma Z} + 2a_e v_e \pm P_e[v_e^2+a_e^2])\kappa^2\left[\frac{Q^2}{Q^2+M_Z^2}\right]^2 xF_3^Z.$$

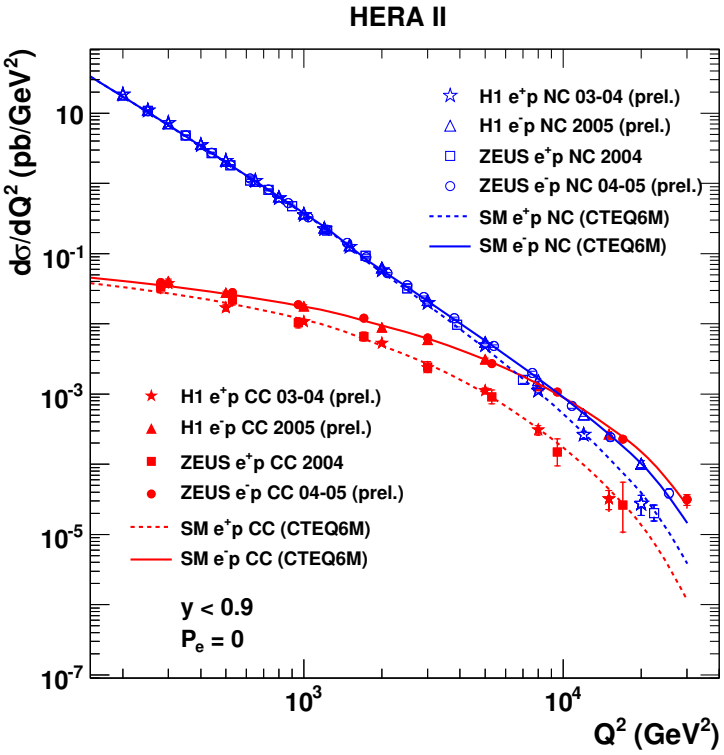

Figure 1: Single-differential cross-sections for $e^{\pm}p$ scattering in neutral current and charged current reactions.

The structure function F_2 corresponds to the case of pure photon exchange. The electron couplings to the Z^0 are denoted by a_e and v_e, P_e is the lepton polarisation and $\kappa^{-1} = \sin^2(2\theta_W)$ is related to the weak mixing angle. The structure functions $F_2^{\gamma Z}$ and $xF_3^{\gamma Z}$ correspond to γ/Z^0 interference effects. The terms related to pure Z^0 exchange are small in the kinematic domain accessible at HERA. In the Born approximation the structure functions can be decomposed into parton density functions (PDFs)

$$\left[F_2, F_2^{\gamma Z}, F_2^Z\right] = \sum_q x\left[e_q^2, 2e_q v_q, (v_q^2 + a_q^2)\right](q + \bar{q}),$$

$$\left[F_3^{\gamma Z}, F_3^Z\right] = \sum_q x\left[2e_q a_q, 2v_q a_q\right](q - \bar{q}).$$

Here e_q, v_q, and a_q are the quark electric charge and couplings to the Z^0 boson. The quark and anti-quark densities of the proton are given by q and $\bar{q}$. The sums run over the five quark flavours $q = \{u, d, s, c, b\}$ accessible at HERA.

1.2 The Charged Current Cross-Section

At Born level the CC cross-section can also be expressed in terms of the parton density functions as follows:

$$\frac{d^2\sigma^{CC}}{dx\,dQ^2}(e^+p \to e^+X) = (1 + P_e)\frac{1}{x}\frac{G_F^2 M_W^4}{4\pi(Q^2 + M_W^2)^2}\left[(1-y)^2(xd + xs + xb) + (x\bar{u} + x\bar{c})\right],$$

$$\frac{d^2\sigma^{CC}}{dx\,dQ^2}(e^-p \to e^-X) = (1 - P_e)\frac{1}{x}\frac{G_F^2 M_W^4}{4\pi(Q^2 + M_W^2)^2}\left[(xu + xc) + (1-y)^2(x\bar{d} + x\bar{s} + x\bar{b})\right].$$

Here G_F is the Fermi constant and M_W is the mass of the W boson.

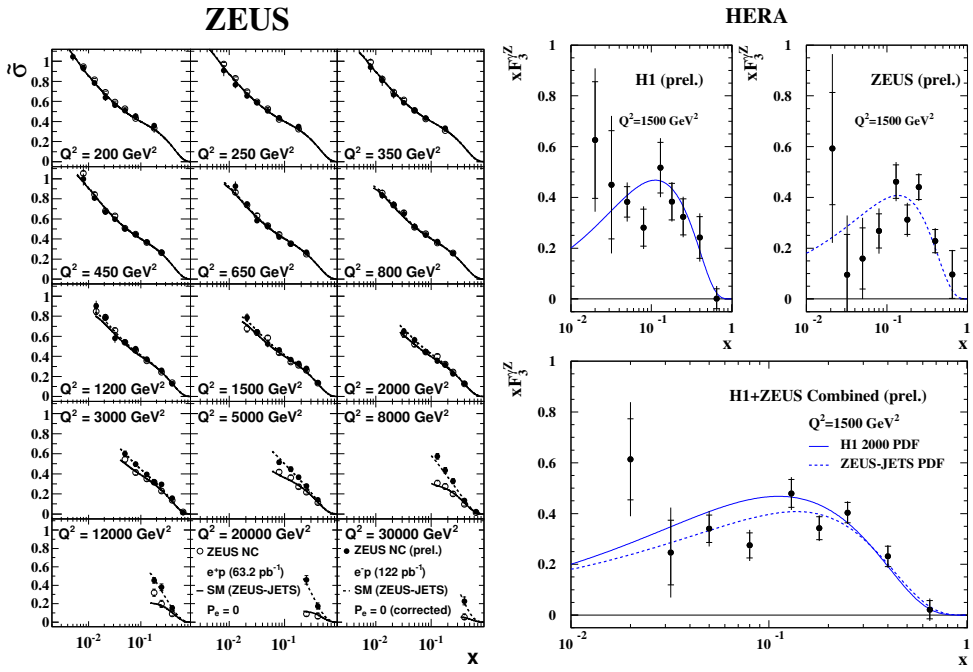

Figure 2: Double-differential cross-sections for $e^{\pm}p$ scattering in neutral current reactions and the resulting measurement of $x\tilde{F}_3$, presented as a function of x for fixed Q^2 values as denoted in the figure.

2 Single-Differential Unpolarised Cross-Sections

The single-differential cross-sections of the NC and CC reactions as a function of Q^2 have been measured by H1 [3,4] and ZEUS [5,6,7]. The results are shown in Figure 1. Compared to HERA I, the precision of the e^-p data has improved significantly. At low Q^2, the NC cross-section is dominated by the photon propagator and behaves like $\frac{1}{Q^4}$. In contrast, the CC cross-section is almost constant at low Q^2. At high Q^2 the NC and CC cross-section are of similar size, a direct way to visualise the electroweak unification at scales near the heavy gauge boson masses. Significant differences between the e^+p and e^-p NC cross-sections are due to the γ/Z^0 interference. For the CC process, the differences between e^+p and e^-p scattering is due to the different types of valence quarks entering the reaction and from the different helicity factors for the valence quarks.

3 Double-Differential Unpolarised Cross-Sections

The double-differential NC cross-section has been measured for e^-p and e^+p collisions. Data from HERA II are combined with HERA I data. The ZEUS data are shown in Figure 2. The difference between the e^-p and e^+p datasets is used to extract [8] the structure function $x\tilde{F}_3$. In order to enhance the statistical precision, the data points are all transformed to $Q^2 = 1500\,GeV$. The combined H1 and ZEUS results on the structure function $xF_3^{\gamma Z}$ are also shown in Figure 2. Using the xF_3 data, the sum rule $\int_0^1 \frac{xF_3}{x}dx = \frac{5}{3}$ can be tested at high Q^2. The experimental result

$$\int_{0.02}^{0.65} \frac{xF_3}{x}dx = 1.21 \pm 0.09(stat) \pm 0.08(sys)$$

is in agreement with expectations from QCD fits and with the sum rule, when extrapolated to $x = 0$ and $x = 1$.

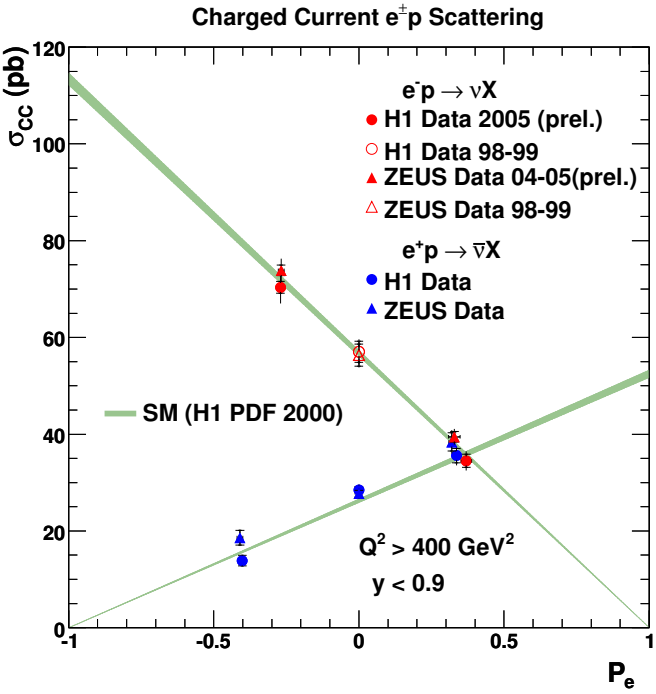

Figure 3: The cross-section integrated up to $y = 0.9$ for $e^{\pm}p$ scattering in charged current reactions as a function of the lepton polarisation, P_e.

Table 1: Right-handed charged current cross-sections derived from the polarisation dependence of the total charged-current cross-section.

e^-p extrapolated to $P_e = 1$	
H1 (prel.)	$-0.9 \pm 2.9_{stat} \pm 1.9_{sys} \pm 2.9_{pol}$
ZEUS (prel.)	$0.8 \pm 3.1_{\text{stat}} \pm 5.0_{\text{sys+pol}}$
e^+p extrapolated to $P_e = -1$	
H1	$-3.9 \pm 2.3_{\text{stat}} \pm 0.7_{\text{sys}} \pm 0.8_{\text{pol}}$

4 Polarised Cross-Sections

4.1 The polarised charged current cross-section

The charged current cross-section predicted by the standard model has a simple linear dependence on the polarisation P_e of the incoming lepton

$$\sigma^{CC}(P_e) = (1 \pm P_e)\, \sigma^{CC}(P_e = 0).$$

Beyond the standard model, there may be a non-vanishing contribution from right-handed charged currents, for example by the exchange of a heavy W_R boson. Figure 3 shows the integrated charged current cross-section for $Q^2 > 400\,GeV$ and $y < 0.9$ as a function of the lepton polarisation, P_e. The data are in good agreement with a linear dependence of σ^{CC} on P_e. If the cross-section is extrapolated to $P_e = +1$ ($P_e = -1$) for incoming electrons (positrons), limits on right-handed charged currents can be set. The limits are summarised in Table 1. If translated to a limit on a massive W_R boson with right-handed couplings of electroweak strength, then W_R masses smaller than 208 GeV are excluded at 95% confidence level (using only the H1 result on polarised e^+p data).

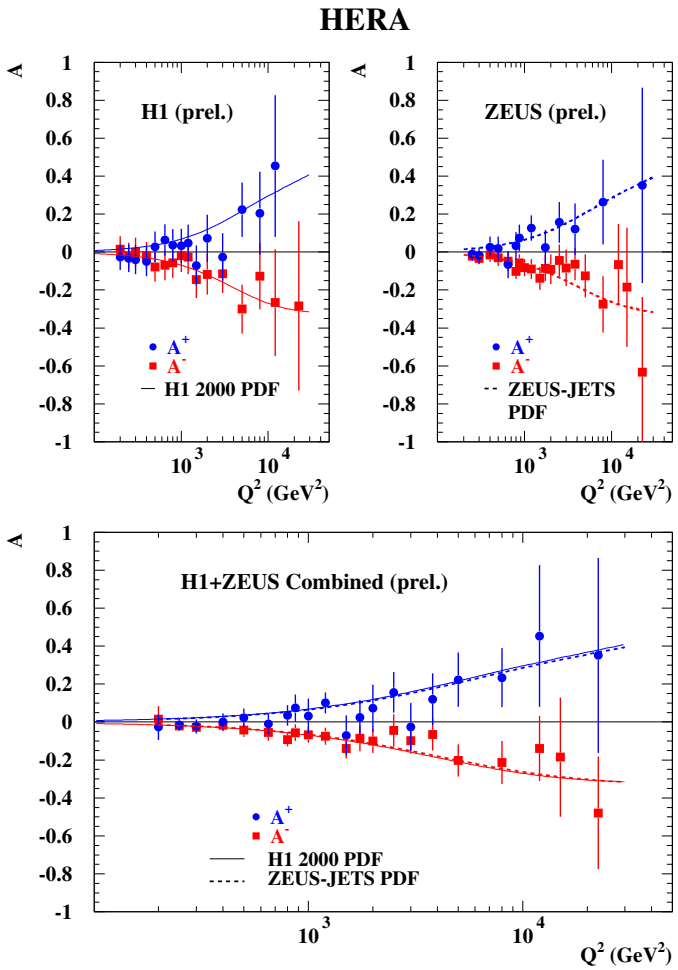

Figure 4: The asymmetry $A^{\pm}(Q^2)$ (see text) as a function of Q^2 for neutral current $e^{\pm}p$ reactions with polarised leptons measured at HERA.

4.2 The polarised neutral current cross-section

The polarised NC cross-sections are different from the unpolarised case due to the parity violating couplings of the Z^0 boson. These are particularly relevant at high Q^2, therefore the difference increases with Q^2. Both H1 and ZEUS have measured the asymmetry

$$A^{\pm} = \frac{2}{P_R - P_L} \frac{\sigma^{\pm}(P_R) - \sigma^{\pm}(P_L)}{\sigma^{\pm}(P_R) + \sigma^{\pm}(P_L)}$$

for $e^{\pm}p$ collisions. Here $P_R > 0$ and $P_L < 0$ denote the lepton polarisation P_e reached by HERA for different setting of the spin-rotators. The combined results are shown in Figure 4. The asymmetry $A^{\pm}$ reaches values of 0.4 for high values of Q^2. The measurements are in good agreement with standard model predictions based on fits of unpolarised data and they provide direct evidence for parity violation mediated by electroweak effects in NC reactions at high Q^2. The asymmetry has a different sign depending on the lepton charge. A^+ and A^- are of similar size, as expected from the Z^0/γ interference term. Note that the asymmetry is sensitive to the quark vector couplings.

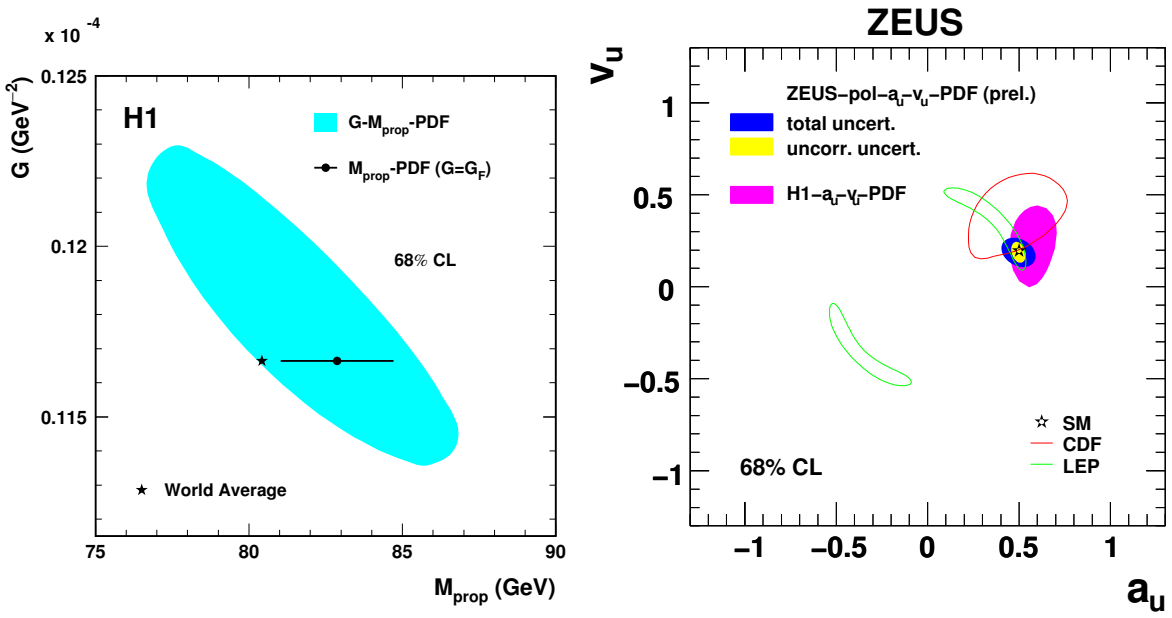

Figure 5: Determination of the W mass and the u quark axial and vector couplings, a_u and v_u, from HERA data.

5 Electroweak Fits

QCD parameters and parton densities have been determined with high precision from HERA data [9,10]. Recently, new fits have been performed where in addition to QCD parameters some electroweak parameters are determined [11,12]. Examples of fits to the W mass and the u quark axial and vector couplings are shown in Figure 5. The precision on the W mass is not competitive to direct measurements at LEP and Tevatron. Still, it is interesting to see that the CC propagator mass measured in ep collisions at high Q^2 is consistent with on-shell measurements performed at other machines. The determination of the u and d quark couplings to the Z^0 improve significantly over the measurements performed at other colliders.

6 Searches for New Physics

6.1 Leptoquarks

Leptoquarks (LQs) are bosons with both leptonic and baryonic quantum numbers. A new quantum number $F = 3B + L$ is introduced. In a generic model developed by Buchmüller Rückl and Wyler [13], LQs are grouped by their electroweak quantum numbers and 14 different types of LQs are accessible at HERA. LQs can be pair-produced in e^+e^- or $p\bar{p}$ collisions. At HERA, LQs can be singly produced from the incoming lepton and a quark from the proton. If the LQ mass is smaller than the HERA centre-of-mass energy, then the LQ is produced on-shell and its mass can be reconstructed using the formula $M = \sqrt{sx}$. For LQ masses beyond the HERA centre-of-mass energy, the Q^2 spectrum is sensitive to the presence of LQs. Inclusive data from deep inelastic scattering at HERA I and HERA II have been searched for LQs [14,15,16] and no signal was found. The reconstructed LQ mass and mass-dependent limits on LQ production determined from HERA II data are shown in Figure 6 for one particular type of LQ. The limits on LQ production depend on the LQ type and mass. For masses of 200 GeV the limit on the LQ coupling is of order 0.02. For couplings of electromagnetic strength ($\lambda = 0.3$) the mass limit is of order 300 GeV.

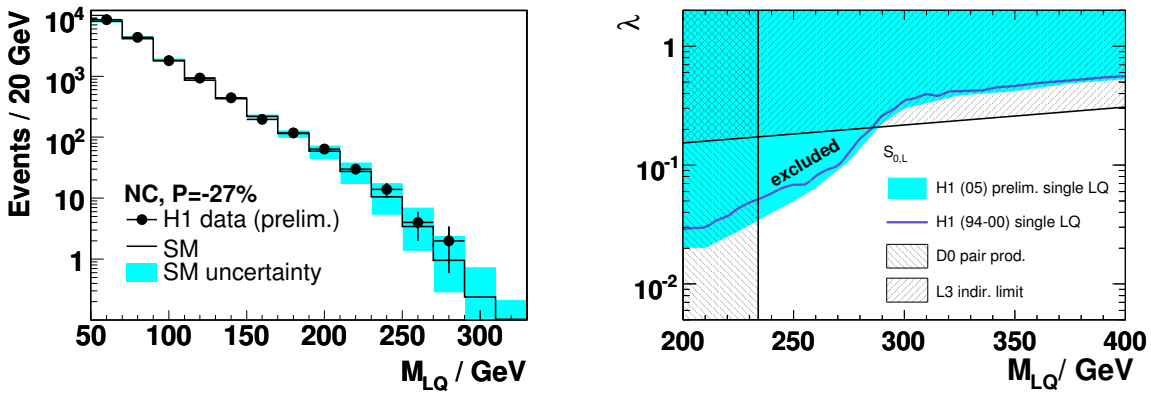

Figure 6: Reconstructed mass M_{LQ} spectrum and the standard model expectation for the leptoquark search and resulting 95% confidence level exclusion limit on the S_{0L} particle as a function of its mass.

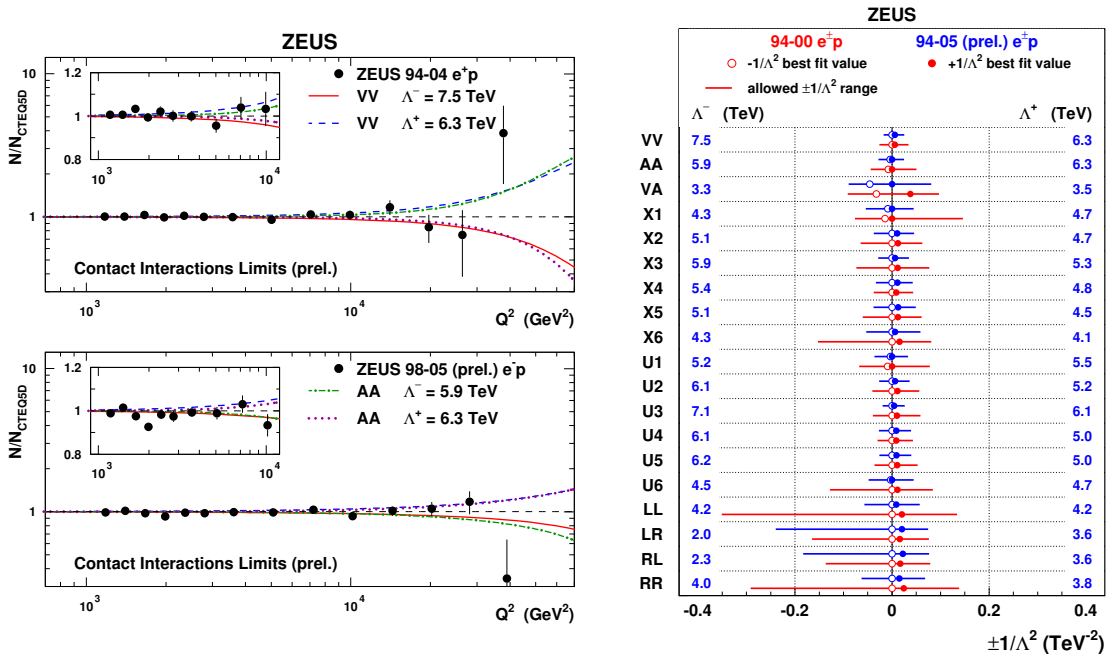

Figure 7: Reconstructed Q^2 spectrum normalised to the SM expectation for the contact interaction search and 95% confidence exclusion limits on various Contact Interaction models.

6.2 Contact interactions

The HERA I and HERA II data have been searched for contact interactions, large extra dimensions and finite quark radii [17,18]. These effects can modify the single-differential cross-sections at high Q^2. No evidence of such phenomena was found and limits have been set. Figure 7 shows the single-differential NC cross-sections as a function of Q^2 normalised to the SM prediction. The expectation from a specific contact interaction model is also shown. Limits are set at 95% confidence on a broad variety of models, as shown in Figure 7. Depending on the model, compositeness scales Λ up to 7.5 TeV are excluded. For models with large extra dimensions, the HERA I+II limit on the mass scale is $M_S > 0.88$ TeV. The limit on the quark radius for point-like electrons is found to be $R_q < 0.67 \times 10^{-16}$ cm.

7 Summary

The HERA collider is a unique facility to measure inclusive $e^{\pm}p$ reactions at high momentum transfer with polarised leptons. The electroweak structure function xF_3 is extracted from neutral current $e^{\pm}p$ reactions. The polarisation dependence of charged current reactions provides an interesting method to look for right-handed charged currents which do not exist in the standard model. For neutral current reactions, the polarisation asymmetry gives direct evidence for parity violating effects at high momentum transfer Q^2. Fits to the inclusive cross-section measurements are made in order to simultaneously extract QCD and electroweak parameters. The HERA results on the u and d quark axial and vector couplings complement the LEP results on heavy quarks. Finally, the inclusive cross-sections are searched for physics beyond the standard model in leptoquark production and contact interactions. No evidence for new physics is found.

References

1. H1 collab, I. Abt *et al*, *Nucl. Instrum. Methods* A**386** (1997) 310 and 348; R. D. Appuhn *et al*, *Nucl. Instrum. Methods* A**386** (1997) 397.
2. ZEUS collab, U. Holm (ed.), unpublished, `http://www-zeus.desy.de/bluebook/bluebook.html`.
3. H1 collab., contributed paper to ICHEP06 (`H1prelim-06-042`).
4. H1 collab., contributed paper to ICHEP06 (`H1prelim-06-041`).
5. ZEUS collab., S. Chekanov *et al*, *Phys. Lett.* B**637** (2006) 210-222.
6. ZEUS collab., contributed paper to ICHEP06 (`ZEUS-prel-06-001`).
7. ZEUS collab., contributed paper to ICHEP06 (`ZEUS0-prel-06-002`).
8. H1 and ZEUS collab., contributed paper to ICHEP06 (`H1prelim-06-142`).
9. H1 collab., C. Adloff *et al.*, *Eur. Phys. J. C* **30** (2003) 1-32.
10. ZEUS collab., S. Chekanov *et al.*, *Eur. Phys. J. C* **42** (2005) 1-16.
11. H1 collab., A. Aktas *et al.*, *Phys. Lett.* B**632** (2006) 35-42.
12. ZEUS collab., contributed paper to ICHEP06 (`ZEUS-prel-06-003`).
13. W. Buchmüller, R. Rückl, D. Wyler, *Phys. Lett.* B**191** (1987) 442-448. Erratum: W. Buchmüller, R. Rückl, D. Wyler, *Phys. Lett.* B**448** (1999) 320.
14. ZEUS collab., S. Chekanov *et al.*, *Phys. Rev.* D**68** (2003).
15. H1 collab., A. Aktas *et al.*, *Phys. Lett.* B**629** (2005) 9-19.
16. H1 collab., contributed paper to ICHEP06 (`H1prelim-06-061`).
17. H1 collab., C. Adloff *et al.*, *Phys. Lett.* B**568** (2003) 35-47.
18. ZEUS collab., contributed paper to ICHEP06 (`ZEUS-prel-06-018`).